Journal of Colloid and Interface Science 554 (2019) 396–403

Contents lists available at ScienceDirect

Journal of Colloid and Interface Science

journal homepage: www.elsevier.com/locate/jcis

Regular Article

Self-standing hollow porous AuPt nanospheres and their enhanced electrocatalytic performance

Haifei Wang [a], Guanhua Lin [b,*], Xiaoqin Li [c], Wensheng Lu [c], Zhengchun Peng [a,*]

[a] Center for Stretchable Electronics and Nanoscale Systems, College of Optoelectronic Engineering, Shenzhen University, Shenzhen 518060, China
[b] Institute for Advanced Study, Shenzhen University, Nanhai Avenue 3688, Nanshan District, Shenzhen 518060, Guang Dong Province, China
[c] Beijing National Laboratory for Molecular Science, Key Laboratory of Colloid, Interface and Thermodynamics, Institute of Chemistry, Chinese Academy of Sciences, Beijing 100190, China

GRAPHICAL ABSTRACT

Schematic illustration and SEM images of the synthesis process of hollow porous AuPt nanospheres.

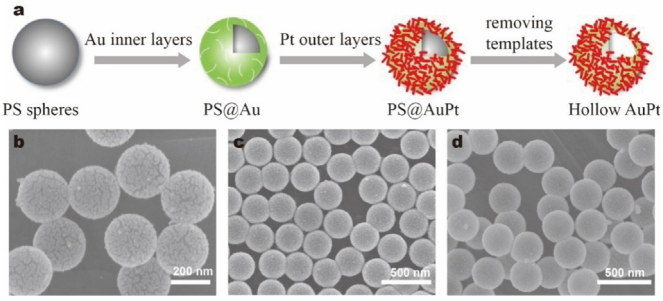

ARTICLE INFO

Article history:
Received 25 March 2019
Revised 29 June 2019
Accepted 9 July 2019
Available online 9 July 2019

Keywords:
Hollow
Porous
AuPt
Nanospheres
Electrocatalytic

ABSTRACT

In this paper, we present a template method to fabricate AuPt hollow nanospheres by depositing Au inner layer and dendritic Pt outer layer onto PS template. The as-prepared AuPt hollow nanospheres can form self-standing hollow nanostructures under thermal treatment which is confirmed by small-angle X-ray scattering results. We believe that the self-standing structural features of them result from different thermal stability of Au and Pt elements. The small-angle X-ray diffraction measurements and X-ray photoelectron spectroscopy of binding energies certify the existing interaction between Au and Pt. It is suggested that Pt mole contents of AuPt hollow nanospheres can be varied by changing H_2PtCl_4 concentration during chemical deposition process. The methanol electrochemical oxidation reaction indicates these as-prepared AuPt hollow nanospheres possessing excellent potential applications on catalysts. Moreover, synthesis of multilayer hollow porous nanospheres such as Pt@Au@Pt proves that our method greatly enriches the species of the self-standing, hollow and porous functional nanomaterials.

1. Introduction

Platinum (Pt) based catalysts are of crucial importance in industrial catalysis, and widely used as the effective heterogeneous catalysts in CO/NO_x oxidation, petroleum refining and fuel cells [1–5]. Therefore, a great deal of efforts has been made on developing

* Corresponding authors.
E-mail addresses: linguanhua01@126.com (G. Lin), zcpeng@szu.edu.cn (Z. Peng).

https://doi.org/10.1016/j.jcis.2019.07.023
0021-9797/

functional Pt nanocatalysts with high catalytic activity, large catalytic reaction areas and good stability. For instance, various shaped nanocatalysts have been fabricated, such as polyhedral [6–8], nanowire [9–11], nanotube [12], nanocages [13–15], core–shell [16–18], mesoporous [19–21], hollow [22,23], dendritic [24], alloy [25,26] and hybrid structures. So far, many Pt based metallic nanocatalysis possessing high electronic conductivity and large surface areas have been prepared, but keeping catalytic activity and preventing aggregation of nanocatalysis is still a big problem, which needs to solve. For example, the commercial Pt catalysts generally were supported on carbon blacks to prevent Pt nanoparticles agglomeration which is helpful in keeping their catalytic activity and stability. However, the corrosion of the carbon supports would lead to Pt aggregation, which results in declining in catalytic activity.

Of them, self-standing porous Pt-based bimetallic nanocatalysts show excellent catalytic activity and stability due to their high specific surface area, efficient transport of reactants and products, solid self-standing structures, and improved utilization efficiency of Pt atoms. It is worth noting that carbon-based supports can be avoided, because their self-standing structure is strong enough for supporting themselves to complete the catalytic process. What's more, Pt based bimetallic hybrids catalysts can increase rates and improve selectivity, which have also attracted considerable attention [27,28]. They are also used in the field of NO_x reduction, CO oxidation, and in electrode reaction for methanol and H_2 fuel cells, their applications as catalyst require the preparation of bimetallic nanostructures uniform in both size and chemical composition [29]. As we known, Pt combined with Au can improve the catalytic activity of Pt by the electronic effect, ensemble effect, and synergistic effect. Here, the synergistic effect means that Pt and Au in the alloys not only present perspective functions but also act cooperatively in the electrocatalysis [30].

There are many efforts for preparation of hollow porous bimetallic catalysts including template methods and galvanic replacement reaction [31,32]. If using polymers, nonionic surfactant [13,33], and peptide conjugates molecules [34] as the templates, which called soft templates, usually need to experience hydrothermal treatment to obtain the hollow nanostructures. Besides, the hollow porous Pt nanostructures also can be prepared by employing the SiO_2 as a hard template and using HF to remove them. However, as HF is a dangerous chemical possessing strong corrosion ability and it also easy damage the deposited metallic layer, which hinder the application of this method [35]. Galvanic replacement reaction also can be used to prepare hollow metallic nanostructures, which usually need more active metal nanostructures reacted with metallic precursor of less active to replace them and their chemical activity was dependent on the metal activity sequence table. So far, numerous shaped hollow Pt based nanostructures have been successfully achieved by using galvanic replacement reaction, such as porous nanotubes [36] and nanospheres [37]. But galvanic replacement reaction is not suitable for fabricating Au@Pt hollow nanostructures due to Au is less active than Pt.

As we known, PS spheres are one of the popular soft templates as their well-controlled size and morphology, easy removal, and wide applications. Herein, we present an effective strategy for design and synthesis of self-standing hollow porous AuPt nanocatalysts with high electrocatalytic activity and good stability based on PS soft templates. Firstly, AuPt hollow nanospheres were prepared by chemical reducing reaction to deposit Au inner layer and dendritic Pt outer layer onto PS nanospheres. Secondly, the self-standing hollow porous AuPt nanospheres were fabricated by solvent thermal treatment methods at 120 °C based on their different thermal stability. Once thermal treatment, Au inner layers were welded into self-standing hollow nanostructures because of its low thermal stability, while Pt outer layers maintain its intrinsic porous structures due to its good thermal stability. The as-prepared nanocatalysts show excellent electrocatalytic performance toward methanol oxidation reaction with high oxidation current density and superior catalytic efficiency. What is more, we also successfully prepared multilayer hollow porous nanospheres such as Pt@Au@Pt. Therefore, we believed that our method can play important role in controllable synthesis of other self-standing, hollow and porous functional metallic nanomaterials.

2. Experimental section

2.1. Materials

PS spheres (about 260 nm in diameter) were used as received. $HAuCl_4$ and H_2PtCl_6 were obtained from Shanghai Reagent Company. Poly (ethyleneimine) branched (PEI, Mn = 10,000) used as polyelectrolyte was purchased from Sigma–Aldrich. Potassium carbonate (K_2CO_3) and reducing agents, formaldehyde (HCHO 37%), sodium borohydride ($NaBH_4$), and ascorbic acid (AA) were received from Beijing Chemical Company. N,N-dimethylformamide (DMF), sulphuric acid (H_2SO_4), Sodium hydroxide (NaOH), methanol (CH_3-OH) and polyvinylpyrrolidone (PVP, Mw = 30,000) were also from the same company. All chemicals were analytical grade and used without further purification. Deionized water used for all experiments were treated with a Millipore water purification system (Millipore Corp.).

2.2. Synthesis of hollow porous AuPt bimetallic Nanospheres

The typical synthesis of hollow porous Au-Pt bimetallic nanospheres was carried out by a two-steps approach. Firstly, Au inner layers and Pt outer layers were deposited onto PS spheres by chemical reduction of their metal precursors respectively. Then, PS spheres were removed in heated DMF to get hollow nanoshells. Here, 5 nm gold nanoparticles were adsorbed on PS nanospheres by electrostatic interaction. Then, Au inner layers were prepared *via* a seeding-mediated growth approach, just followed by soaking as-prepared gold nanoparticle modified PS spheres into 20 mL growth solution, which contained $HAuCl_4$ (0.38 mM), K_2CO_3 (1.0 mM) and PVP (1.0 g/mL). After 2 h, the sample was rinsed thoroughly with deionized water. Pt outer layers were prepared after Au inner layers. 20 mL H_2PtCl_6 (0.228 mM) solution used as metal precursors and 0.5 mL AA (0.10 M) used as reducing agent, PVP (1.0 mg/mL) used as protect agent. PS polymer nanospheres were removed in heated N,N-Dimethyl-formamide (DMF) at temperature of 120 °C for 12 h.

2.3. Characterizations

Electrochemical investigations were performed using a CHI 760D electrochemical analyzer (Chenhua Co., Shanghai, China) with a conventional three-electrode cell system. Cyclic voltammograms (CVs) experiments were performed using an Ag/AgCl (saturated KCl) electrode as a reference electrode, a Pt wire as a counter electrode. And the working electrode was a glassy carbon electrode (GCE, 3 mm in diameters) coated with equal amount of catalysts. 5 μL of samples and 3 μL of 0.5 wt% nafion aqueous solution were subsequently dropped onto the surface of GCE and dried at room temperature before electrochemical experiments. The CV experiments were carried out at a scan rate 100 mV/s and the potential range varied from −0.2 to 1.1 V (*vs.* Ag/AgCl) in a N_2-saturated 0.5 M H_2SO_4 solution. The electrochemically active surface area (ECSA) of a catalyst was determined by measuring the charge amount collected in the hydrogen adsorption/desorption region

between −0.2 V and 0.2 V and assuming the value of adsorption of a hydrogen monolayer is 210 μC/cm^2. Methanol electrooxidation measurements were carried out in solution containing 0.5 M H_2SO_4 and 0.5 M methanol at a scan rate 50 mV/s within the potential range from 0 to 1 V.

The size, morphology and interior structure of catalysts were investigated using field emission scanning electron microscope (SEM, HITACHI S-4800) with an accelerating voltage at 10 kV, transmission electron microscope (JEOLJEM 1011) with an accelerating voltage at 100 kV and a JEM-2100F operating at 200 kV equipped with an energy dispersive spectrometer (EDS) for analyses. X-ray photoelectron spectroscopy (XPS) measurements were conducted in a VG Scientific ESCALab220i-XL spectrometer. Power X-ray diffraction (XRD) measurements were recorded on an EMPYREAN Diffractometer system with monochromatized Cu Kα radiation (λ = 1.5418 Å). Small-angle X-ray scattering (SAXS) measurements were carried out at 298 K on a beam line 4B9A synchrotron radiation X-ray small angle system at Beijing Synchrotron Radiation Facility. Nitrogen adsorption-desorption isotherms were recorded using a micromeritic ASAP2020M+C accelerated surface area and porosimetry analyzers at 77 K. UV–Vis spectra measurements were characterized on U-2800 (400–1100 nm).

3. Results and discussions

Using PS nanospheres as the template to prepare hollow porous metallic nanostructures is one of the typical and traditional strategies due to its numerous advantages. However, making the as-prepared hollow porous nanostructures self-standing is challenge as they are easy collapsed during the process of removing templates. Herein, we presented a layer-by-layer chemical deposition of metallic layers approach to obtain hollow porous AuPt nanospheres at common temperature and usual condition. As illustrated in Fig. 1, Au inner layers could be uniformly deposited onto PS nanospheres, the homogenous porous Pt outer layers were also successfully deposited by using non-ionic surfactants structure-directing agent [38]. Subsequently, well-defined hollow porous AuPt bimetallic nanospheres prepared after thermal treatment at 120 °C to remove PS templates. It could be seen from SEM images (Fig. 1c and d) that the AuPt metallic layer is not damaged, even their particle sizes no noticeable change after experiencing thermal treatment. Their average diameters are determined as 300 nm and 295 nm, respectively. These results suggested that Au and Pt atoms generated specific structures, which are strong enough for supporting them forming self-standing structure. We believed that the self-standing structural features of AuPt hollow porous nanospheres result from different thermal stability of Au and Pt elements. When there is only one element deposited on PS spheres, Au can form well-defined hollow nanospheres after thermal treatment [39], but Pt would generate collapsed structures (Fig. S1). It is because Au nanoparticles possessing low thermal stability under 120 °C, they would weld and interconnect to be united structures [40]. But Pt nanoparticles are thermal stable under 120 °C, which would not fuse to form interconnected and self-standing hollow structures until higher thermal treatment temperature [41]. Even if Au and Pt nanoparticles co-deposited, the as-prepared AuPt hollow structures would collapse after 120 °C thermal treatments (Fig. S2) as Pt nanoparticles could prevent the welding of Au nanoparticles [42], which proved that welding of Au nanoparticles during thermal treatments plays an important role in forming self-standing AuPt hollow porous structures as their stability would increase comparing with the sample without heating (Fig. S3). It also indicates that separately depositing Au and Pt layer is necessary to produce AuPt hollow nanospheres.

Typical transmission electron microscopy (TEM) images of AuPt bimetallic nanoshells are presented in Fig. 2. The centre of the AuPt nanospheres after solution thermal treatment (Fig. 2b) are brighter than before (Fig. 2a), which suggested that the polymer templates are fully removed and porous hollow structures formed. TEM image of broken spheres (Fig. S4a) further confirm the interior of Au-Pt bimetallic nanospheres is empty after thermal treatment, and it can be seen from Fig. 2c that the thickness of hollow nanospheres is ~18 nm. As presented in Fig. 2c, there are gaps between composed AuPt nanostructures, which results in the AuPt nanospheres becoming porous structures. All these results proved that our method successfully fabricates self-standing hollow porous AuPt nanospheres. For further characterization of hollow porous AuPt nanospheres, they were broken under high power ultrasound to investigate the structure of Au inner layer and Pt outer layer by using high magnification TEM. The outer layer is dendritic as seen in high magnification TEM images (Fig. S4b and c). Also, we can see some small nanoparticles attached onto the inner surface, as shown in Fig. 2d, which clearly indicates the feature of double layer. Fig. 2e and Fig. S4d present high magnification TEM (HRTEM) images of Pt dendritic outer layer, their lattice spacing is matched

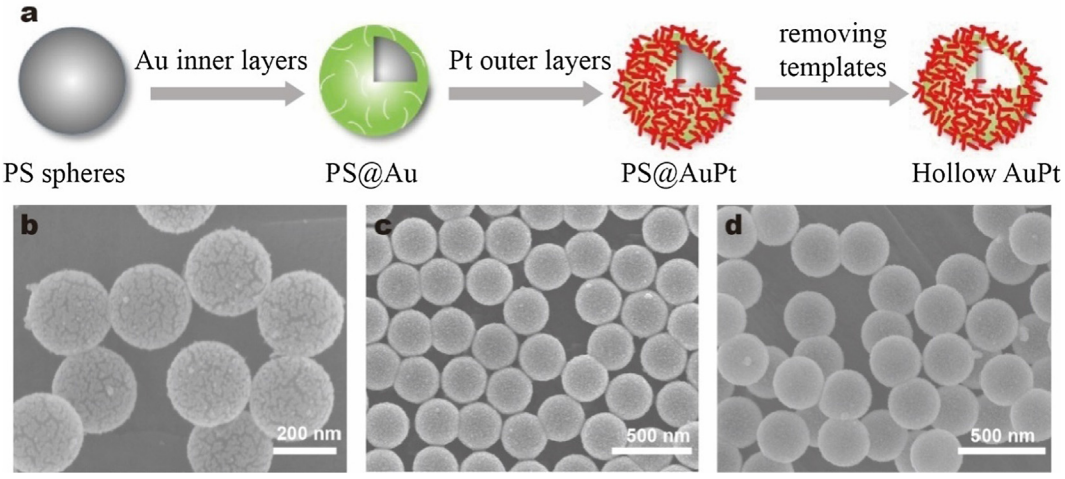

Fig. 1. (a) Schematic illustration of the synthesis process of hollow porous AuPt nanospheres; (b–d) SEM images of (b) PS@Au, (c) PS@AuPt and (d) hollow porous AuPt nanospheres.

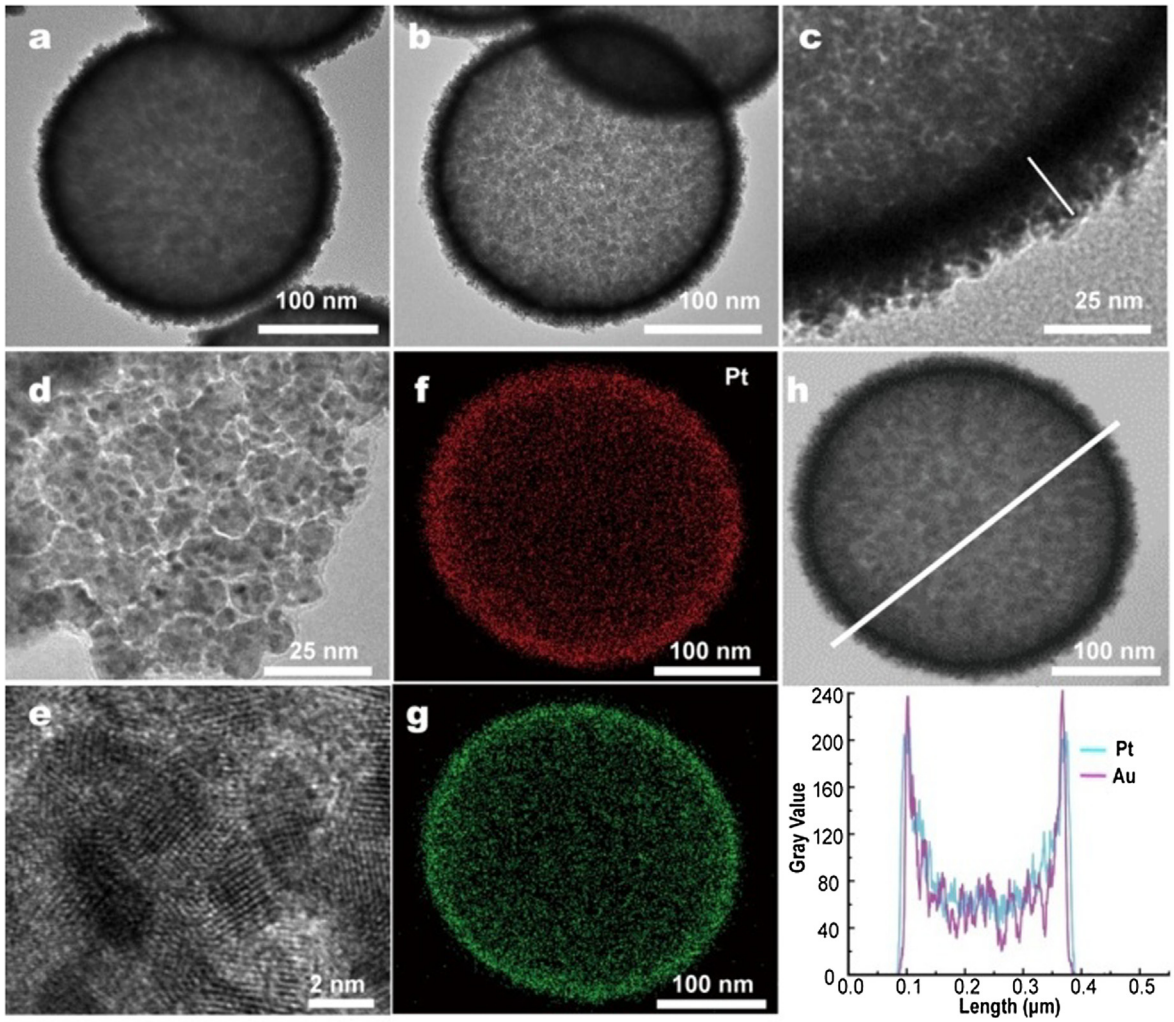

Fig. 2. TEM images of (a) PS@AuPt nanostructures and (b) hollow porous AuPt nanostructures; (c) and (d) highly magnified TEM images of hollow porous AuPt nanostructures; (e) high resolution TEM image of nanoshells of hollow porous AuPt nanostructures; (f) and (g) elemental mapping images of the distribution of Pt (red) and Au (green); (h) scanning TEM image and line-scan profiles recorded from the individual hollow porous AuPt nanostructure. (For interpretation of the references to color in this figure legend, the reader is referred to the web version of this article.)

with (1 1 1) lattice spacing of Pt face-centered cubic (fcc) crystals and they are randomly oriented over the entire area, presenting polycrystalline feature of Pt outer layer. Energy-dispersive X-ray analysis (EDX) maps of the Au and Pt distributions of hollow porous AuPt nanospheres are presented in Fig. 2f and g. The result shows that both Au and Pt atoms are distributed uniformly throughout the whole sphere. A line scanning result (Fig. 2h) reveals that the AuPt nanospheres are double-layered hollow structure including Au inner layer and Pt outer layer.

The size, morphology and structure of the AuPt nanospheres can be well controlled by changing the reaction conditions. As our previous reports, the coverage of Au layer on polymer template is related with the structural features of hollow nanospheres [39]. Interestingly, if changing the volume of Au growth solution (from 5 mL, 7.5 mL to 10 mL) and keep Pt precursor amount (0.190 mM, 20 mL) to prepare Pt outer layer, although uniform AuPt nanospheres were fully covered on polymer templates, the fabricated AuPt nanospheres collapsed when the Au growth solution decreased to 5.0 mL (Fig. S5). It is because there are no enough Au nanoparticles for welding in order to support the self-standing hollow structures. Hence, the nanowelding of Au inner layer under solvent thermal treatment is essential for forming self-standing hollow nanospheres.

Amount of Pt precursor also have influence on the structural features of dendritic outer layer. Here, Au inner layer was deposited by wet chemical reduction with the same amounts of growth solution (10 mL, 0.38 mM), but Pt outer layers were deposited in 30 mL Pt precursor solution. As presented in Fig. 3, the thickness of Pt dendritic outer layer increase and the hollow structure of nanospheres are still well reserved when amount of Pt precursor increased. In addition, element mapping images reveal that Au and Pt were still uniformly distributed throughout the entire nanospheres at this moment (Fig. 3). Thus, thickness of Pt outer layer is controllable by varying Pt precursor amount. And the EDS results show that Pt mole contents of nanospheres are 36.1%, 44.9% and 46.2%, respectively. It means that increasing the concentration of Pt precursor also can perfectly enhance the Pt content in the AuPt nanospheres within certain degree. In contrast, when the Pt precursors were decreased lower than 0.076 mM, nanospheres collapsed after thermal treatment (Fig. S6). Although the Pt outer layer is not the dominate factors for forming hollow nanospheres, It also can enhance the metallic layer coverage of nanospheres, which is crucial for forming self-standing hollow nanospheres as literature reported [39]. The depositions of Pt outer layer on Au inner layer were characterized by UV–vis spectroscopy (Fig. S7). Au inner layers show a broad absorption peak at 750 nm, which

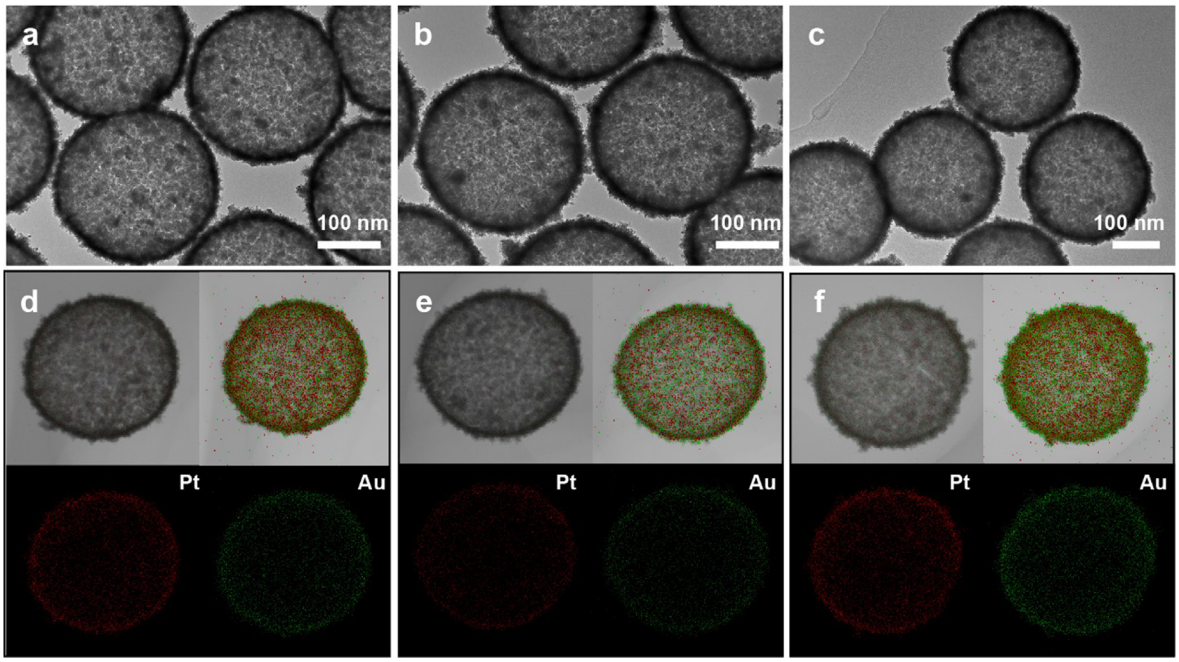

Fig. 3. (a–c) Are typical TEM images of different types of hollow porous AuPt nanostructures with different Pt fractions. (d–f) Are scanning TEM images and elemental mapping images of distribution of Pt (red) and Au (green) with different Pt fractions. Pt precursor concentration is (a and d) 0.152 mM, (b and e) 0.190 mM and (c and f) 0.228 mM, respectively. (For interpretation of the references to color in this figure legend, the reader is referred to the web version of this article.)

were due to the surface plasmon resonance of closely packed Au nanoparticles of inner layer. When Pt outer layer was deposited, a red-shift and broaden absorption peak was observed [16], and the more Pt deposited, the broader of absorption peak varied from 800 nm to 1100 nm. These results confirmed that increasing the concentration of Pt precursor can enhance the Pt mole content in the AuPt nanospheres.

Small-angle X-ray scattering (SAXS) measurements of as prepared AuPt nanospheres were used to study their mesoscale structural information. The SAXS patterns of AuPt nanospheres and Au nanospheres after thermal treatment clearly show ring type diffraction features (Fig. 4a). The corresponding SAXS integral curves exhibit more than 14 diffraction peaks, suggested that these nanospheres are good accordance with the feature of hollow particles [43]. However, the SAXS integral curve of Pt nanospheres shows no typical diffraction peaks of hollow particles (Fig. 4a), indicated they collapsed after thermal treatment. Therefore, the SAXS results present obvious evidences on the feature of hollow nanostructures.

For further characterization of their porous structural feature of as prepared bimetallic nanospheres. The small-angle XRD measurements of PS@AuPt nanospheres, hollow AuPt nanospheres and hollow Au nanospheres were carried on. As expected, Au hollow nanospheres show no peaks, but PS@AuPt and hollow AuPt nanospheres present broad peaks at $2\theta = 1.35$ and $2\theta = 1.74$ (Fig. 4b), which indicated formation of mesoporous structure attributed to the closely packed Pt dendritic outer layers. The d spacing values were calculated to be 6.5 nm and 5.2 nm by using formula $d = \frac{\lambda}{2\sin\theta}$. In addition, the interface interaction of Au and Pt proved through XPS spectra. As shown in Fig. 5, the binding

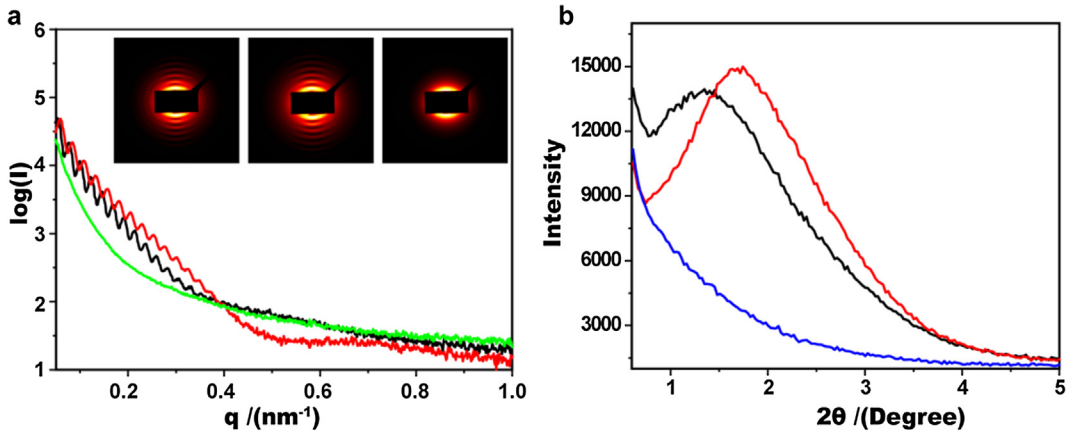

Fig. 4. (a) Small-angle X-ray scattering integral curves of hollow Au nanoshells (red line), hollow porous AuPt nanoshells (black line) and Pt nanoparticles (green line), respectively; the insets show SAXS patterns of hollow Au nanoshells (left), hollow porous AuPt nanoshells (middle) and Pt nanoparticles (right), respectively. (b) Small-angle XRD patterns of PS@AuPt nanoshells (red line), hollow AuPt nanoshells (black line) and hollow Au nanoshells (blue line), respectively. (For interpretation of the references to color in this figure legend, the reader is referred to the web version of this article.)

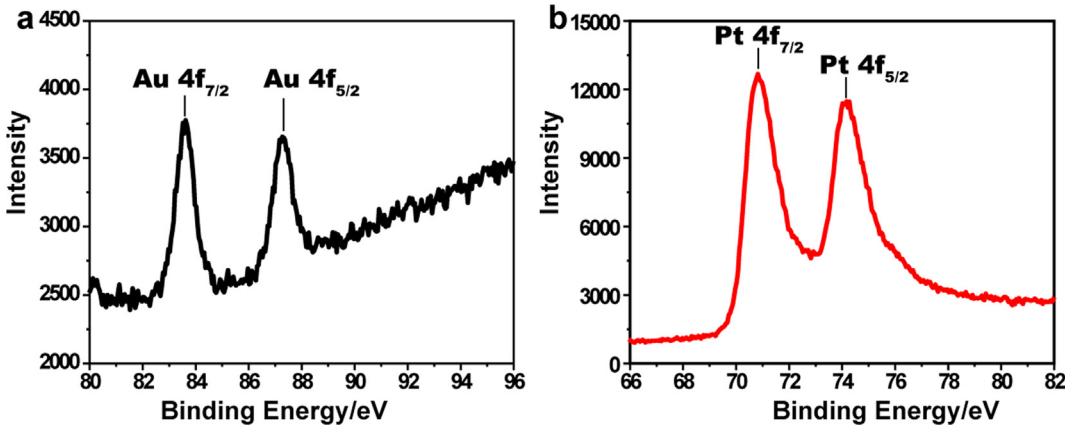

Fig. 5. (a) and (b) X-ray photoelectron spectroscopy (XPS) spectra of Au 4f (a) and Pt 4f (b) of hollow porous AuPt nanostructures.

energies of Pt $4f_{7/2}$ and Pt $4f_{5/2}$ at 70.8 eV and 74.2 eV, and the binding energies of Au$4f_{7/2}$ and Au $4f_{5/2}$ at 83.6 eV and 87.3 eV, respectively. Compared with monometallic Au (Au $4f_{7/2}$, 84.0 eV) and Pt (Pt$4f_{7/2}$, 71.0 eV), the negative shift of binding energies is ascribed to interaction between Au and Pt [44,45]. Furthermore, according to the results of nitrogen absorption isotherms (Fig. S8), specific surface area of hollow porous AuPt bimetallic nanospheres is 36.1 m^2/g. Therefore, the distinctive structural features of self-standing hollow porous AuPt nanospheres show good reaction areas, which implied excellent potential applications on catalysts.

With the unique structural features, the hollow porous self-standing AuPt nanospheres were investigated by electrocatalytic reaction. The electrochemical active surface areas (ECSAs) were calculated using cyclic voltammetry measurements in a 0.5 M H_2SO_4 solution at room temperature with a scan rate 100 mV/s. The ECSA is theoretically calculated by integrating the charges of hydrogen adsorption/desorption between −0.2 V and 0.2 V. As shown in Fig. 6a, hollow porous AuPt nanospheres showed higher specific ECSA (39.9 m^2/g) than commercial Pt/C catalyst (22.3 m^2/g). The methanol electrochemical oxidation reaction was carried out in an aqueous solution containing 0.5 M H_2SO_4 and 0.5 M CH_3OH. The cyclic voltammograms (CV) profiles were recorded by sweeping from 0 V to 1 V (*versus* Ag/AgCl) at a scan rate 50 mV/s. As shown in Fig. 6b, the two anodic peaks were observed both on the forward and backward sweeps, indicated the electrochemical oxidation process of methanol. In comparison with the commercial Pt catalysts (Fig. S9), hollow porous AuPt nanospheres demonstrated a higher current density for methanol electrooxidation. The methanol oxidation current density of hollow porous AuPt nanospheres is 0.66 mA/cm^2, which is ~300% higher than that of the commercial Pt black catalyst. In addition, the peak potentials of methanol electrooxidation are 0.7 V and 0.43 V for the forward and backward sweeps, respectively. The onset potential of hollow porous AuPt nanospheres is much smaller than that of commercial Pt black catalysts in both forward and backward sweeps. The results further confirm that as-prepared hollow porous AuPt nanospheres possess better catalytic activity than that of commercial Pt black catalyst. Moreover, they exhibit higher I_f/I_b ratio (~1.4) (in which I_f and I_b are the forward and backward current densities, respectively) than that of commercial Pt black catalyst, proved their superior catalytic efficiency for fully methanol electro oxidation. For further test the stability of their catalytic performances, long-term current-time (I-t) response of methanol electrooxidation was carried out at a constant voltage of 0.65 V for 800 s (Fig. 6c). The results demonstrated that the current density of hollow porous AuPt nanospheres is higher than that of commercial Pt black catalyst. In addition, the decay time of electrochemical current for the methanol oxidation reaction on hollow porous AuPt nanospheres is longer than that on commercial Pt black catalysts. These results further reveal that hollow porous AuPt nanospheres exhibit better superior electrochemical stability and higher electrocatalytic performance on the methanol oxidation reaction. Moreover, hollow porous AuPt nanospheres also show higher electrochemical activity for methanol oxidation reaction in alkaline media (Fig. S10).

The observed good enhancements on electrochemical performance of hollow porous AuPt nanospheres could be ascribed to their special structural features. (a) Good electrochemical reaction interface: hollow interior and porous structures facilitate them diffusion/transport of electrochemical reagents, the self-standing nanostructures enhance structural stability for avoiding aggregation and porous Pt dendritic nanoshells provide large active

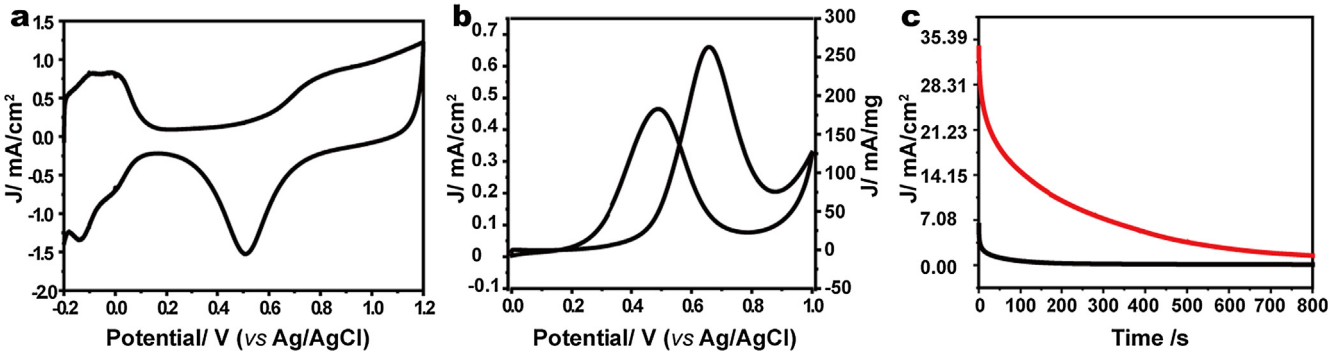

Fig. 6. Electrochemical measurements of hollow porous AuPt nanostructures in (a) 0.5 M H_2SO_4 solution at a scan rate 100 mV/s and (b) in 0.5 M H_2SO_4 + 0.5 M CH_3OH solution at a scan rate 50 mV/s; (c) Current density–time curves of hollow porous AuPt nanostructures in 0.5 M H_2SO_4 + 0.5 M CH_3OH solution at 0.65 V.

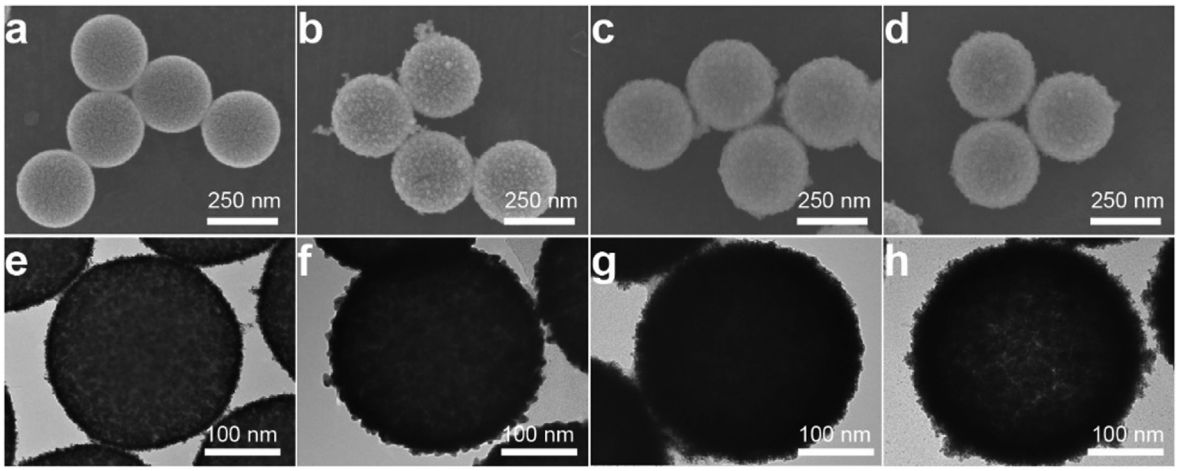

Fig. 7. SEM and TEM images of (a and e) PS@Pt, (b and f) PS@Pt@Au, (c and g) PS@Pt@Au@Pt and (d and h) hollow porous Pt@Au@Pt, respectively.

surfaces. (b) High electrocatalytic activity: the interconnected Au inner layers are beneficial for electron transport to active sites, the synergetic effects of bimetallic nanospheres are considered to enhance catalytic activity. In addition, the self-standing nanospheres exhibit intrinsic advantages, which avoid supporting corrosion problem faced by commercial catalysts. Therefore, we expand this concept to prepare multilayer hollow porous nanospheres such as Pt@Au@Pt by depositing Pt inner layer, Au middle layer and Pt outer layer successively (Fig. 7). It can be seen from TEM image that Pt@Au@Pt nanospheres also possess self-standing, hollow and porous structural features. Significantly, we believed that our method greatly enriches the species of the self-standing, hollow and porous functional nanomaterials.

In summary, we present an effective and promising strategy for design and synthesis of bimetallic self-standing and hollow porous nanocatalysts with high electrocatalytic activity. The self-standing hollow porous AuPt nanospheres were successfully fabricated by combining chemical deposition metallic nanostructures layer-by-layer and solvent thermal treatment methods to remove soft templates. Under thermal treatment, formation of self-standing hollow nanostructures depends on nanowelding of Au inner layers and Pt outer layers maintain its intrinsic porous structures, because of their different thermal stability. The as-prepared AuPt nanospheres show excellent electrocatalytic performance toward the methanol oxidation reaction, with high oxidation current density and superior catalytic efficiency. The enhancements on electrochemical performance are ascribed to the special features of hollow porous structures and the synergetic effect of bimetallic composites, indicated promising potential applications in fuel cells.

Declaration of Competing Interest

The authors declare no competing financial interest.

Acknowledgements

This work was supported by National Natural Science Foundation of China (61671308 and 21773259), Department of Education of Guangdong Province (2016KZDXM005) and Natural Science Foundation of Guangdong Province (2018A030310552).

Appendix A. Supplementary material

TEM and SEM images, UV-vis spectroscopy and N_2 adsorption-desorption isotherm of AuPt hollow spheres, and electrochemical measurements of Pt black and hollow porous AuPt nanostructures. This material is available free of charge *via* Internet. Supplementary data to this article can be found online at https://doi.org/10.1016/j.jcis.2019.07.023.

References

[1] M.V. Twigg, Catalytic control of emissions from cars, Catal. Today 163 (2011) 33–41.
[2] B.C. Steele, A. Heinzel, Materials for fuel-cell technologies, Nature 414 (2001) 345–352.
[3] M.K. Debe, Electrocatalyst approaches and challenges for automotive fuel cells, Nature 486 (2012) 43–51.
[4] T.P. Vispute, H. Zhang, A. Sanna, R. Xiao, G.W. Huber, Renewable chemical commodity feedstocks from integrated catalytic processing of pyrolysis oils, Science 330 (2010) 1222–1227.
[5] R.J. Davis, E.G. Derouane, A non-porous supported-platinum catalyst for aromatization of n-hexane, Nature 349 (1991) 313.
[6] J. Wu, L. Qi, H. You, A. Gross, J. Li, H. Yang, Icosahedral platinum alloy nanocrystals with enhanced electrocatalytic activities, J. Am. Chem. Soc. 134 (2012) 11880–11883.
[7] Y. Wu, D. Wang, X. Chen, G. Zhou, R. Yu, Y. Li, Defect-dominated shape recovery of nanocrystals: a new strategy for trimetallic catalysts, J. Am. Chem. Soc. 135 (2013) 12220–12223.
[8] B.Y. Xia, H.B. Wu, X. Wang, X.W. Lou, Highly concave platinum nanoframes with high-index facets and enhanced electrocatalytic properties, Angew. Chem. Int. Ed. 52 (2013) 12337–12340.
[9] L. Ruan, E. Zhu, Y. Chen, Z. Lin, X. Huang, X. Duan, Y. Huang, Biomimetic synthesis of an ultrathin platinum nanowire network with a high twin density for enhanced electrocatalytic activity and durability, Angew. Chem. Int. Ed. 52 (2013) 12577–12581.
[10] B.Y. Xia, H.B. Wu, Y. Yan, X.W. Lou, X. Wang, Ultrathin and ultralong single-crystal platinum nanowire assemblies with highly stable electrocatalytic activity, J. Am. Chem. Soc. 135 (2013) 9480–9485.
[11] K. Jiang, Q. Shao, D. Zhao, L. Bu, J. Guo, X. Huang, Phase and composition tuning of 1D Platinum-Nickel nanostructures for highly efficient electrocatalysis, Adv. Funct. Mater. 27 (2017) 1700830.
[12] L. Chen, L. Kuai, X. Yu, W. Li, B. Geng, Advanced catalytic performance of Au-Pt double-walled nanotubes and their fabrication through galvanic replacement reaction, Chem.-Eur. J. 19 (2013) 11753–11758.
[13] L. Wang, Y. Yamauchi, Metallic nanocages: synthesis of bimetallic Pt-Pd hollow nanoparticles with dendritic shells by selective chemical etching, J. Am. Chem. Soc. 135 (2013) 16762–16765.
[14] C. Chen, Y. Kang, Z. Huo, Z. Zhu, W. Huang, H.L. Xin, J.D. Snyder, D. Li, J.A. Herron, M. Mavrikakis, M. Chi, K.L. More, Y. Li, N.M. Markovic, G.A. Somorjai, P. Yang, V.R. Stamenkovic, Highly Crystalline multimetallic nanoframes with three-dimensional electrocatalytic surfaces, Science 343 (2014) 1339–1343.
[15] H. Fan, M. Cheng, Z. Wang, R. Wang, Layer-controlled Pt-Ni porous nanobowls with enhanced electrocatalytic performance, Nano Res. 10 (2017) 187–198.
[16] H. Ataee-Esfahani, L. Wang, Y. Nemoto, Y. Yamauchi, Synthesis of bimetallic Au@Pt nanoparticles with Au Core and nanostructured Pt shell toward highly active electrocatalysts, Chem. Mater. 22 (2010) 6310–6318.
[17] H. Ataee-Esfahani, L. Wang, Y. Yamauchi, Block copolymer assisted synthesis of bimetallic colloids with Au core and nanodendritic Pt shell, Chem. Commun. 46 (2010) 3684–3686.
[18] L. Wang, Y. Yamauchi, Autoprogrammed synthesis of triple-layered Au@Pd@Pt core–shell nanoparticles consisting of a Au@Pd bimetallic core and nanoporous Pt shell, J. Am. Chem. Soc. 132 (2010) 13636–13638.

[19] C. Li, M. Imura, Y. Yamauchi, Displacement plating of a mesoporous Pt skin onto Co nanochains in a low-concentration surfactant solution, Chem. - Eur. J. 20 (2014) 3277–3282.
[20] C. Li, B. Jiang, M. Imura, V. Malgras, Y. Yamauchi, Mesoporous Pt hollow cubes with controlled shell thicknesses and investigation of their electrocatalytic performance, Chem. Commun. 50 (2014) 15337–15340.
[21] B.K. Pilapil, J. van Drunen, Y. Makonnen, D. Beauchemin, G. Jerkiewicz, B.D. Gates, Ordered porous electrodes by design: toward enhancing the effective utilization of platinum in electrocatalysis, Adv. Funct. Mater. 27 (2017) 1703171.
[22] H. Lee, J.-A. Kwak, D.-J. Jang, Laser-Induced fabrication of hollow platinum nanospheres for enhanced catalytic performances, J. Phys. Chem. C 118 (2014) 22792–22798.
[23] Q. Lu, C. Wei, L. Sun, Z.A. Alothman, V. Malgras, Y. Yamauchi, H. Wang, L. Wang, Smart design of hollow AuPt nanospheres with a porous shell as superior electrocatalysts for ethylene glycol oxidation, RSC Adv. 6 (2016) 19632–19637.
[24] S.J. Guo, J. Li, S.J. Dong, E.K. Wang, Three-dimensional Pt-on-Au bimetallic dendritic nanoparticle one-step, high-yield synthesis and its bifunctional plasmonic and catalytic properties, J. Phys. Chem. C 114 (2010) 15337–15342.
[25] W. Liu, D. Haubold, B. Rutkowski, M. Oschatz, R. Hübner, M. Werheid, C. Ziegler, L. Sonntag, S. Liu, Z. Zheng, A.-K. Herrmann, D. Geiger, B. Terlan, T. Gemming, L. Borchardt, S. Kaskel, A. Czyrska-Filemonowicz, A. Eychmüller, Self-supporting hierarchical porous PtAg alloy nanotubular aerogels as highly active and durable electrocatalysts, Chem. Mater. 28 (2016) 6477–6483.
[26] L. Zhang, L.-X. Ding, H. Chen, D. Li, S. Wang, H. Wang, Self-supported PtAuP alloy nanotube arrays with enhanced activity and stability for methanol electro-oxidation, Small 13 (2017) 1604000.
[27] C. Li, H. Tan, J. Lin, X. Luo, S. Wang, J. You, Y.-M. Kang, Y. Bando, Y. Yamauchi, J. Kim, Emerging Pt-based electrocatalysts with highly open nanoarchitectures for boosting oxygen reduction reaction, Nano Today 21 (2018) 91–105.
[28] C. Li, M. Iqbal, J. Lin, X. Luo, B. Jiang, V. Malgras, K.C.W. Wu, J. Kim, Y. Yamauchi, Electrochemical deposition: an advanced approach for templated synthesis of nanoporous metal architectures, Acc. Chem. Res. 51 (2018) 1764–1773.
[29] A.M. Landry, E. Iglesia, Synthesis of bimetallic AuPt clusters with clean surfaces via sequential displacement-reduction processes, Chem. Mater. 28 (2016) 5872–5886.
[30] J. Liu, L. Cao, W. Huang, Z. Li, Preparation of AuPt alloy foam films and their superior electrocatalytic activity for the oxidation of formic acid, ACS Appl. Mater. Interfaces 3 (2011) 3552–3558.
[31] V. Malgras, H. Ataee-Esfahani, H. Wang, B. Jiang, C. Li, K.C.-W. Wu, J.H. Kim, Y. Yamauchi, Nanoarchitectures for mesoporous metals, Adv. Mater. 28 (2016) 993–1010.
[32] X. Wang, J. Feng, Y. Bai, Q. Zhang, Y. Yin, Synthesis, properties, and applications of hollow Micro-/Nanostructures, Chem. Rev. 116 (2016) 10983–11060.
[33] H. Ataee-Esfahani, M. Imura, Y. Yamauchi, All-metal mesoporous nanocolloids: solution-phase synthesis of core-shell Pd@Pt nanoparticles with a designed concave surface, Angew. Chem. Int. Ed. 52 (2013) 13611–13615.
[34] C. Song, Y. Wang, N.L. Rosi, Peptide-directed synthesis and assembly of hollow spherical CoPt nanoparticle superstructures, Angew. Chem. Int. Ed. 52 (2013) 3993–3995.
[35] H. Wang, H.Y. Jeong, M. Imura, L. Wang, L. Radhakrishnan, N. Fujita, T. Castle, O. Terasaki, Y. Yamauchi, Shape- and size-controlled synthesis in hard templates: sophisticated chemical reduction for mesoporous monocrystalline platinum nanoparticles, J. Am. Chem. Soc. 133 (2011) 14526–14529.
[36] S.M. Alia, G. Zhang, D. Kisailus, D. Li, S. Gu, K. Jensen, Y. Yan, Porous platinum nanotubes for oxygen reduction and methanol oxidation reactions, Adv. Funct. Mater. 20 (2010) 3742–3746.
[37] H.P. Liang, H.M. Zhang, J.S. Hu, Y.G. Guo, L.J. Wan, C.L. Bai, Pt hollow nanospheres: facile synthesis and enhanced electrocatalysts, Angew. Chem. Int. Ed. 43 (2004) 1540–1543.
[38] X. Teng, X. Liang, S. Maksimuk, H. Yang, Synthesis of porous platinum nanoparticles, Small 2 (2006) 249–253.
[39] H. Wang, J. Han, W. Lu, J. Zhang, J. Li, L. Jiang, Facile preparation of gold nanocages and hollow gold nanospheres via solvent thermal treatment and their surface plasmon resonance and photothermal properties, J. Colloid Interface Sci. 440 (2015) 236–244.
[40] M. Ding, D.C. Sorescu, G.P. Kotchey, A. Star, Welding of gold nanoparticles on graphitic templates for chemical sensing, J. Am. Chem. Soc. 134 (2012) 3472–3479.
[41] S. Mandal, M. Sathish, G. Saravanan, K.K.R. Datta, Q. Ji, J.P. Hill, H. Abe, I. Honma, K. Ariga, Open-mouthed metallic microcapsules: exploring performance improvements at agglomeration-free interiors, J. Am. Chem. Soc. 132 (2010) 14415–14417.
[42] Y. Ding, M. Chen, J. Erlebacher, Metallic mesoporous nanocomposites for electrocatalysis, J. Am. Chem. Soc. 126 (2004) 6876–6877.
[43] D.I. Svergun, K. Mhj, Small-angle scattering studies of biological macromolecules in solution, Rep. Prog. Phys. 66 (2003) 1735.
[44] J. Zeng, J. Yang, J.Y. Lee, W. Zhou, Preparation of carbon-supported core-shell Au-Pt nanoparticles for methanol oxidation reaction: the promotional effect of the Au core, J. Phys. Chem. B 110 (2006) 24606–24611.
[45] Y. Yamauchi, A. Tonegawa, M. Komatsu, H. Wang, L. Wang, Y. Nemoto, N. Suzuki, K. Kuroda, Electrochemical synthesis of mesoporous Pt-Au binary alloys with tunable compositions for enhancement of electrochemical performance, J. Am. Chem. Soc. 134 (2012) 5100–5109.